Supporting information for "Radium Sorption to Iron (hydr)oxides, Pyrite, and Montmorillonite: Implications for Mobility"

Authors:

Michael A. Chen

Benjamin D. Kocar

Number of Pages: 21

Number of Figures: 8

Number of Tables: 4

Experimental Methods: Ferrihydrite naturally exists as a hydrated mineral,[1] thus it was important to prepare and handle the mineral such that its hydration was preserved. Here, a ferrihydrite slurry was synthesized by adding 0.4 M NaOH to a 50 mM ferric chloride hexahydrate solution, and then centrifuging and washing the resulting precipitate three times with 18 MΩ water, resulting in a thick paste of ferrihydrite. A small volume (<100 mL) of DI water was added to create a slurry consistency. The iron content of the prepared ferrhydrite slurry was determined through colorimetry (ferrozine method)[2] and stirred slurry aliquots were added directly to the experiments to achieve the desired mineral mass.

Goethite was prepared through slow air-oxidation of a 50 mM Fe^{2+} and 100 mM bicarbonate solution over two days, and then centrifuged and washed three times with 18 MΩ water. The resultant slurry was then oven dried at 70 °C for two hours, resulting in a mineral powder that was then gently ground with a mortar and pestle to homogenize the sample. This dried sample was added directly to experimental bottles.

There are well established methods for preparing natural clay mineral samples for use in experimental work.[3] The STx-1b montmorillonite ordered from the Clay Minerals Society was originally a calcium montmorillonite, but was converted to sodium montmorillonite for easier comparison to other studies. This was achieved by first dispersing the clay with 1 M NaCl, then siphoning the suspended <0.2 µm clay fraction by successively centrifuging and suspending the clay eight times in DI water. The suspension was flocculated with saturated NaCl, and excess solution removed via centrifugation. The clay suspension was then treated with a 1 M sodium acetate solution (pH 5) to remove residual carbonate minerals. The resulting Na-equilibrated montomorillonite was then centrifuged and equilibrated with the experimental background solution (10 mM NaCl), centrifuged again, dried at 70 °C overnight, and then gently powdered

using mortar and pestle. This dried powder was added directly to the experiments. Results of the kinetic experiments involving sodium montmorillonite are shown in figure S1, showing that over a 24 hour period, the water Ra concentrations stabilize.

All prepared minerals' surface area was measured using a BET surface area analyzer (table S1). Ferrihydrite was dried for this analysis, and pyrite was held anaerobically until analysis.

Displacement of H^+ from mineral surfaces can cause sorption experiments to drift in pH over time, requiring some pH adjustment. Following the experimental period (24 hours), pH was checked and re-titrated to the desired value if necessary; if the pH deviated more than 0.1 pH units, the bottle was allowed to re-equilibrate for 15 minutes after titration, and the re-titration process repeated. This process was sufficient to ensure the experimental pHs described.

The composition of the various background solutions used in sorption experiments are reported in table S2. Artificial groundwater, brackish water, and seawater were diluted from a 2x artificial seawater stock. The ratio of individual cations was not selected to match a specific location, but rather to simulate common groundwater and seawater cations in "typical" environmental ratios.[4] The cations selected for single competing cation experiments reported in figure 2 of the main text were selected based on the composition of the artificial waters. Only chloride salts of these cations were used to make solutions to limit interference from different anions.

Control experiments without any mineral were also performed to examine Ra sorption to the serum bottle surface. Some pH dependent sorption was observed, but was limited in comparison to the minerals studied. Given the limited observed sorption within controls, no corrections to data were made. Serum bottles and caps were scrubbed in detergent solution,

rinsed, soaked in 2% HNO_3 for at least 1 hour, rinsed 3 times with 18 MΩ water, and then air dried before usage in experiments. This procedure was sufficient to prevent Ra and mineral cross contamination across experiments.

Analytical Methods: Background concentrations Ra were measured through scintillation counting (N = 47) to develop a limit of blank of 1.4 counts per second (cps). From this, we developed a blank derived minimum detection limit of 0.209 Bq, as defined by the EPA (EPA 821-R-16-006).[5] A Canberra low energy germanium detector and multichannel analyzer was calibrated using a multinuclide standard from Eckert and Ziegler (www.ezag.com), and ^{226}Ra activities for scintillation counting standards were determined using Canberra Genie software using the 186 keV peak.

Comparison of Sorption Experiment Results: Fitted K_d and K_{sa} values developed from isotherm experiments are reported in table S1, with the corresponding fits plotted for each mineral in figure S2. Errors reported for K_d values are the standard error of regression produced by the least squares fitting function, `linregress`, from the python package SciPy, and K_{sa} the fitted K_d normalized by mineral specific surface area. These values were also used for error bar plots in the main text (figure 1). The pH and pH error are the average and standard deviation of all data points used for a given regression.

Our results are compared with literature K_d values (Table S3), which are mostly derived from experimental isotherms. In some cases, a K_d value was not reported, thus a K_d value was fit directly from the reported experimental data. The greatest number of reported Kd values are found for the iron (hydr)oxides; however, there are significant differences in the experimental conditions (solid-solution loading, background electrolyte composition, etc.). Notable similarities and differences are explained in the main text.

Surface Complexation Modeling: Experimental sorption data was fit by varying Ra sorption reaction constants.[6,7] Surface area and site densities, while fittable parameters in the models, were not varied, and were constrained with surface areas reported in table S1 and site densities previously determined in the literature (table S4). For exchange sites used montmorillonite modeling, the CEC value given by the The Clay Minerals Society (clays.org) was used. Solution complexation behavior was accounted for using the SIT database, which includes Ra carbonate, sulfate, chloride, and hydroxide complexes, albeit these solution complexes had little impact over the experimental conditions considered.

The surface complexes used to model Ra sorption and impact of competing ions are reported in table S4. Ra complexation constants were fitted to match sorption isotherm data or circumneutral, varied background cation data, and are also reported for both methods of fitting in table S4. The resultant visual fits to the isotherm data are shown in figures S3, S4, and S5, using the typical means of comparing the isotherm pH vs the fraction of Ra sorbed, and plotting both the SCM result and the experimental data. For fitting the competiting cation data, another approach was used, where data points are plotted by their experimental value, and the value produced by the SCM (Figures S6, S7, and S8). To evalulate the whole fit, the RMSE of the simulation results vs the experimental data was calculated, and is reported in the main text. As discussed in the main text, the log K values generated using either fitting method were also evaluated using the complimentary method, as plotted in the supplementary figures S3-S8. Constants for the other surface complexes are drawn from the literature, however many of the models used in the literature use alternative representations of the mineral surface (ie. CD-MUSIC, or extended triple layer models), thus the constants are not readily applicable to the

generalized two layer models used here. Only constants fit using the same type of mineral specific model and similar surface complexes were used to model background electrolyte competition. Carbonate surface complexes were only included in the SCM for goethite, as the goethite synthesis method involves high concentrations of carbonate to buffer pH, resulting in carbonate surface complexes that persist even after washing.[8] Some cations used experimentally (e.g. Na^+, K^+) did not have published constants, but clearly demonstrated differential amounts of sorption (Figure 2, main text, Figures S6, S7, S8). In these cases, no constants were fit or used, underscoring a potential limitation for using these models for predicting Ra transport in natural systems.

We also considered a few other mineral-specific SCMs to attempt replication of results reported in the main text. For the Fe (hydr)oxides, single site models featuring tetradentate surface coordination have been used in both generalized double layer models, and extended triple layer models to fit divalent cation sorption.[7,9,10] For montmorillonite, many models have been proposed, but no standardized SCM has been adopted, some which follow the non-electrostatic method used here, others using various means of representing the permanent negative charge of the clay surface.[11,12] While in some cases use of these models improved fits to our data, the lack of spectroscopic studies for Ra combined with the limited database of constants for competing ions effectively precluded the use of these alternative models. The non-standardization of these different SCMs and their calibration also impeded any efforts to test their viability for predicting transport of Ra in the different geochemical conditions tested here.[13] Thus, we elected to use relatively "simple" models that are well established in the literature, and have a wider variety of available reaction constants that can be used to model the effect of different competing cations. In the case of pyrite, no model specific to an unoxidized surface was available, and testing a few

different reactions with free Ra did not produce satisfactory fits. A previous SCM used to model Eu and Sr sorption to pyrite used both unoxidized and oxidized sites to replicate experimental data, but that model did not fit here either.[14] Additionally, since there is no experimental evidence of oxidation of the pyrite surface, a model that included such types of sites would be inappropriate. That these simpler models failed to provide meaningful prediction of the impact of different solution conditions (main text), and the no models were able to fit the pyrite experimental data found here suggests that further detailed study of Ra sorption to mineral surfaces is needed to constrain these SCMs. In particular, constants to explain the differences in Na and K sorption, as well as better understanding of mineral specific Ra surface complexes would improve these models' predictive capability.

Table S1. Mineral Surface Areas and Fitted K_d and K_{sa} values

Mineral	Surface Area (m^2/g)	pH	K_d (mL/g)	K_{sa} (mL/m^2)
Ferrihydrite	383	3	405±72	1.06±0.19
		5	526±48	1.37±0.13
		7	2420±210	6.33±0.55
		9	302000±29000	789±76
Goethite	146	3	2.77±7.86	0.019±0.054
		5	400±42	2.73±0.29
		7	679±52	4.64±0.36
		9	12400±700	84.8±4.8
Sodium Montmorillonite	50.2	3	7740±860	154±17
		5	20000±2000	398±40
		7	22600±300	451±6
		9	25400±1500	507±29
Pyrite	0.07	3	156±18	2280±260
		5	400±29	5840±420
		7	579±16	8450±230
		9	574±29	8380±430

Table S2: Major Salt Concentrations in the different background treatments

Experiment	Na (mM)	K (mM)	Mg (mM)	Ca (mM)	Sr (mM)	Cl (mM)
NaCl	10					10
KCl		10				10
$MgCl_2$			10			20
$CaCl_2$				10		20
$SrCl_2$					10	20
AGW	5	2	0.5	0.5	0.0001	9
ABW	50	20	5	5	0.001	90
ASW	400	160	40	40	0.008	720

Table S3. Comparison of Literature Ra Sorption Experiments and Fitted Kd Values

Mineral	Solid/Solution Ratio (mg/L)	Background Solution	pH	Kd (mL/g)	Source
Ferrihydrite	300	10 mM NaCl	7	2420	This study
	300	10 mM NaCl	9	302000	This study
	25000	Seawater	8.25	1535	[15]
	10000	100 mM $NaClO_4$	7	1440	[7]
Goethite	300	10 mM NaCl	3	2.77	This study
	300	10 mM NaCl	5	400	This study
	300	10 mM NaCl	7	679	This study
	300	10 mM NaCl	9	12400	This study
	25000	Seawater	8.25	20	[15]
	10000	100 mM $NaClO_4$	7	50.6	[7]
	500000	"pH 1 solution"	1	0.752	[16]
	500000	"pH 10 solution"	10.1	544	[16]
Lepidocrocite	25000	Seawater	8.25	174	[15]
Hematite	25000	Seawater	8.25	75	[15]
Sodium Montmorillonite	300	10 mM NaCl	5	20000	This study
	300	10 mM NaCl	7	22600	This study
	3333	10 mM NaCl	5.25	9700	[17]
	50000	10 mM NaCl	6.5	3724	[18]

158 **Table S4: Surface complexation reactions and constants from data fitting**

Reactions	Sites (mol/g)	log K Isotherm	Lg K Salinity	Source
Ferrihydrite				
Protonation		7.92	7.92	A
$\equiv Fhy_sOH + H^+ \rightleftarrows \equiv Fhy_sOH_2^+$	1.87E-3	-8.93	-8.93	A
$\equiv Fhy_sOH \rightleftarrows \equiv Fhy_sO^- + H^+$		7.92	7.92	A
$\equiv Fhy_wOH + H^+ \rightleftarrows \equiv Fhy_wOH_2^+$	4.67E-5	-8.93	-8.93	A
$\equiv Fhy_wOH \rightleftarrows \equiv Fhy_wO^- + H^+$				
Radium				Fitting
$\equiv Fhy_sOH + Ra^{2+} \rightleftarrows \equiv Fhy_sOHRa^{2+}$		6.7	5.7	Fitting
$\equiv Fhy_wOH + Ra^{2+} \rightleftarrows \equiv Fhy_wORa^+ + H^+$		-2.8	-11.0	Fitting
$\equiv Fhy_wOH + Ra^{2+} + H_2O \rightleftarrows \equiv Fhy_wORaOH + 2H^+$		-15	-9.4	
Competing Ions				A
$\equiv Fhy_sOH + Ca^{2+} \rightleftarrows \equiv Fhy_sOHCa^{2+}$		4.97	4.97	A
$\equiv Fhy_wOH + Ca^{2+} \rightleftarrows \equiv Fhy_wOCa^+ + H^+$		-5.85	-5.85	A
$\equiv Fhy_wOH + Mg^{2+} \rightleftarrows \equiv Fhy_wOMg^+ + H^+$		4.6	4.6	A
$\equiv Fhy_sOH + Sr^{2+} \rightleftarrows \equiv Fhy_sOHSr^{2+}$		5.01	5.01	A
$\equiv Fhy_wOH + Sr^{2+} \rightleftarrows \equiv Fhy_wOSr^+ + H^+$		-6.58	-6.58	A
$\equiv Fhy_wOH + Sr^{2+}\ H_2O \rightleftarrows \equiv Fhy_wOSrOH + 2H^+$		-17.6	-17.6	
Goethite				
Protonation				
$\equiv GoeOH + H^+ \rightleftarrows \equiv GoeOH_2^+$	4.87E-4	6.93	6.93	B
$\equiv GoeOH \rightleftarrows \equiv GoeO^- + H^+$		-9.65	-9.65	B
Radium				
$\equiv GoeOH + Ra^{2+} \rightleftarrows \equiv GoeORa^+ + H^+$		-3.9	-2.5	Fitting
$\equiv GoeOH + Ra^{2+} \rightleftarrows \equiv GoeOHRa^{2+}$		3.5	-6.6	Fitting
Competing Ions				
$\equiv GoeOH + Ca^{2+} \rightleftarrows \equiv GoeOCa^+ + H^+$		-6.48	-6.48	B
$\equiv GoeOH + Ca^{2+} \rightleftarrows \equiv GoeOHCa^{2+}$		3.98	3.98	LFER, B
$\equiv GoeOH + Mg^{2+} \rightleftarrows \equiv GoeOMg^+ + H^+$		-3.02	-3.02	B
$\equiv GoeOH + Mg^{2+} \rightleftarrows \equiv GoeOHMg^{2+}$		5.24	5.24	LFER, B
$\equiv GoeOH + Sr^{2+} \rightleftarrows \equiv GoeOSr^+ + H^+$		-5.44	-5.44	B
$\equiv GoeOH + Sr^{2+} \rightleftarrows \equiv GoeOHSr^{2+}$		3.59	3.59	LFER, B
$\equiv GoeOH + 2H^+ + CO_3^{2-} \rightleftarrows \equiv GoeOCOOH + H_2O$		20.78	20.78	C
$\equiv GoeOH + H^+ + CO_3^{2-} \rightleftarrows \equiv GoeOCOO^- + H_2O$		12.71	12.71	C
Sodium Montmorillonite				
Exchange				
$2 \equiv Clay\text{-}Na + Ra^{2+} \rightleftarrows \equiv Clay_2\text{-}Ra + 2\ Na^+$	8.45E-4	0.2	0.2	Fitting, D
$2 \equiv Clay\text{-}Na + Ca^{2+} \rightleftarrows \equiv Clay_2\text{-}Ca + 2\ Na^+$		0.5	0.5	E
$2 \equiv Clay\text{-}Na + Mg^{2+} \rightleftarrows \equiv Clay_2\text{-}Mg + 2\ Na^+$		0.4	0.4	F
Surface Protonation				
$\equiv Clay_sOH + H^+ \rightleftarrows \equiv Clay_sOH_2^+$	2E-6	4.5	4.5	G

$\equiv Clay_sOH \rightleftarrows \equiv Clay_sO^- + H^+$		-7.9	-7.9	G
$\equiv Clay_{w1}OH + H^+ \rightleftarrows \equiv Clay_{w1}OH_2^+$	4E-5	4.5	4.5	G
$\equiv Clay_{w1}OH \rightleftarrows \equiv Clay_{w1}O^- + H^+$		-7.9	-7.9	G
$\equiv Clay_{w2}OH + H^+ \rightleftarrows \equiv Clay_{w2}OH_2^+$	4E-5	6.0	6.0	G
$\equiv Clay_{w2}OH \rightleftarrows \equiv Clay_{w2}O^- + H^+$		-10.5	-10.5	G
Radium				
$\equiv Clay_sOH + Ra^{2+} \rightleftarrows \equiv Clay_sORa^+ + H^+$		0.0	-0.9	Fitting
$\equiv Clay_{w1}OH + Ra^{2+} \rightleftarrows \equiv Clay_{w1}ORa^+ + H^+$		-2.1	-1.9	Fitting
Competing Ions				
$\equiv Clay_sOH + Mg^{2+} \rightleftarrows \equiv Clay_sOMg^+ + H^+$		-2.4	-2.4	LFER, H
$\equiv Clay_{w1}OH + Mg^{2+} \rightleftarrows \equiv Clay_{w1}OMg^+ + H^+$		-5.2	-5.2	LFER, H
$\equiv Clay_sOH + Ca^{2+} \rightleftarrows \equiv Clay_sOCa^+ + H^+$		-3.4	-3.4	LFER, H
$\equiv Clay_{w1}OH + Ca^{2+} \rightleftarrows \equiv Clay_{w1}OCa^+ + H^+$		-5.2	-5.2	LFER, H
$\equiv Clay_sOH + Sr^{2+} \rightleftarrows \equiv Clay_sOSr^+ + H^+$		-3.9	-3.9	LFER, H
$\equiv Clay_sOH + Sr^{2+} + H_2O \rightleftarrows \equiv Clay_sOSrOH + 2H^+$		-16.7	-16.7	LFER, H
$\equiv Clay_{w1}OH + Sr^{2+} \rightleftarrows \equiv Clay_{w1}OSr^+ + H^+$		-6.8	-6.8	LFER, H
$\equiv Clay_{w1}OH + Sr^{2+} + H_2O \rightleftarrows \equiv Clay_{w1}OSrOH + 2H^+$		-20.8	-20.8	LFER, H

Notes: LFER: Indicates constants was fitted using a linear free energy relationship from the denoted source. Sources: A: From Dzombak and Morel, 1990.[19] B: From Mathur and Dzombak, 2006.[20] C: From Van Geen, Robertson, and Leckie, 1994.[21] D: Number of exchange sites from CEC reported by Clays.org for STx-1b Calcium Montmorillonite. Exchange reaction fitted to match low pH sorption (ie, sorption without surface site impacts). E: From Tournassat et al., 2004.[22] F: From Charlet and Tournassat, 2005.[23] G: From Bradbury and Baeyens, 1997.[24] H: From Bradbury and Baeyens, 2005.[25]

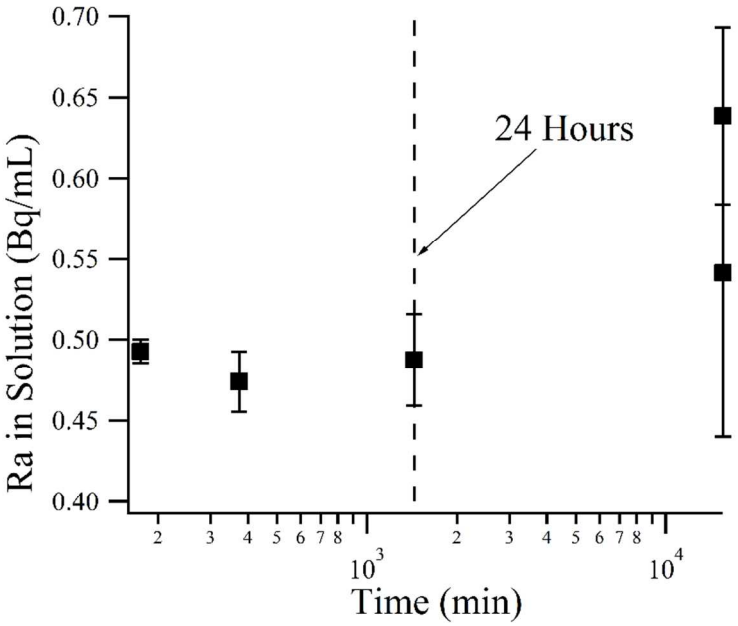

167 Figure S1. Ra sorption to Sodium Montmorillonite as a function of time.

168

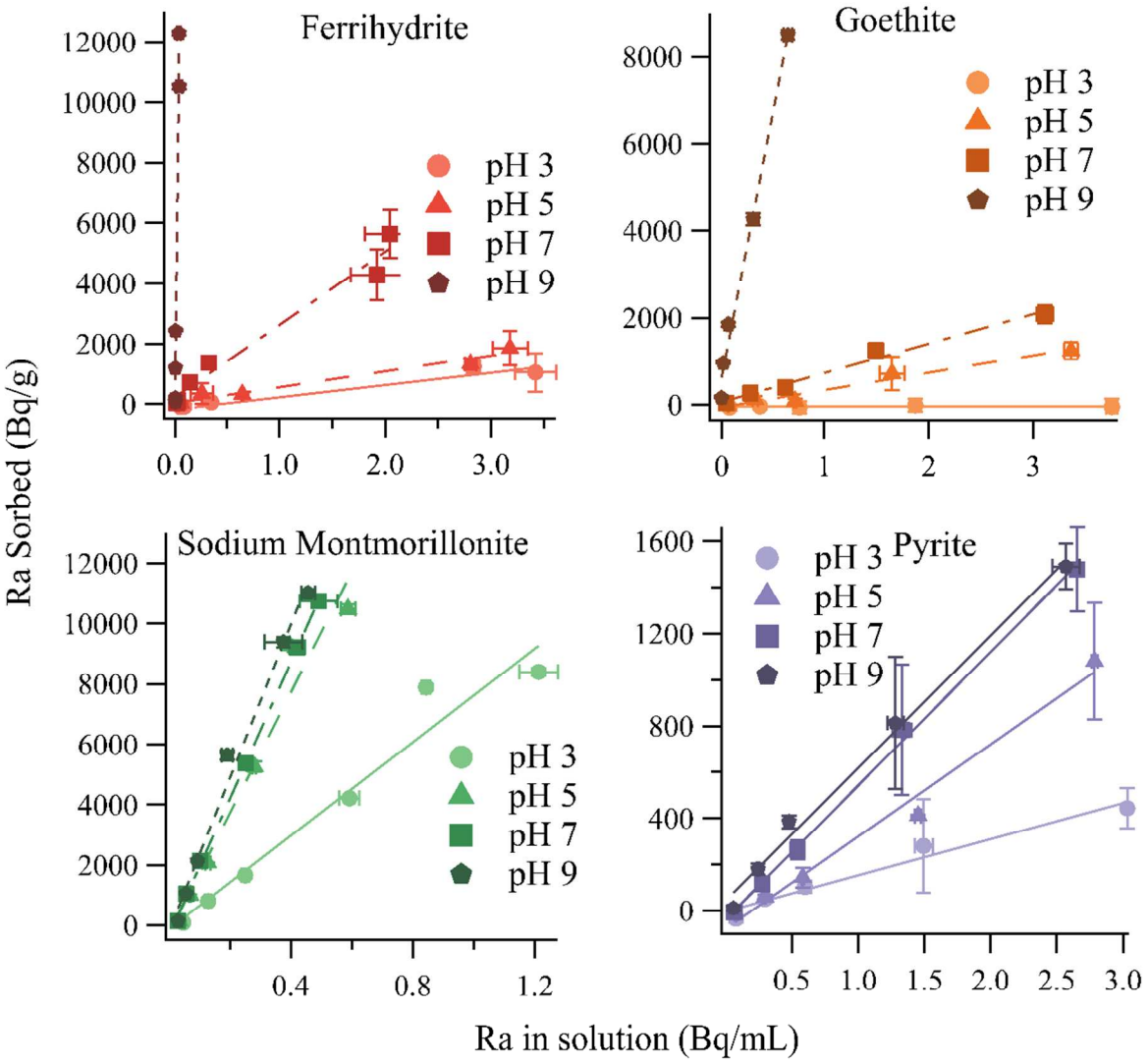

Figure S2: Results of isotherm experiments with linear fits.

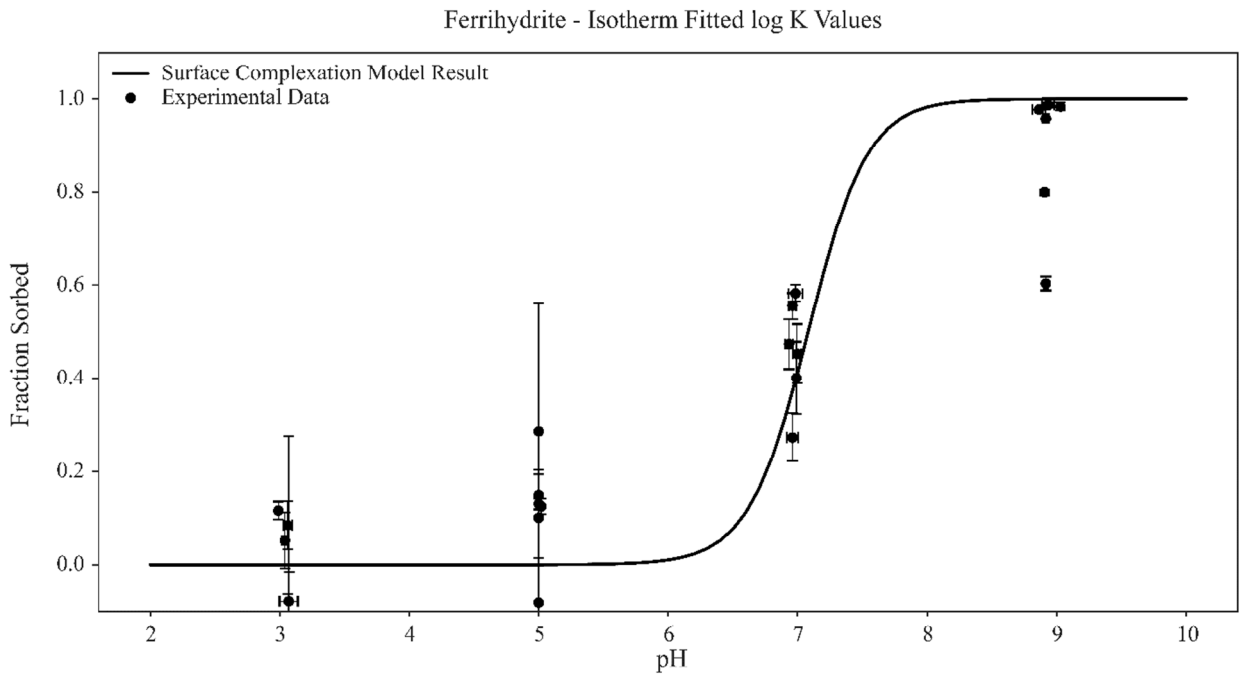

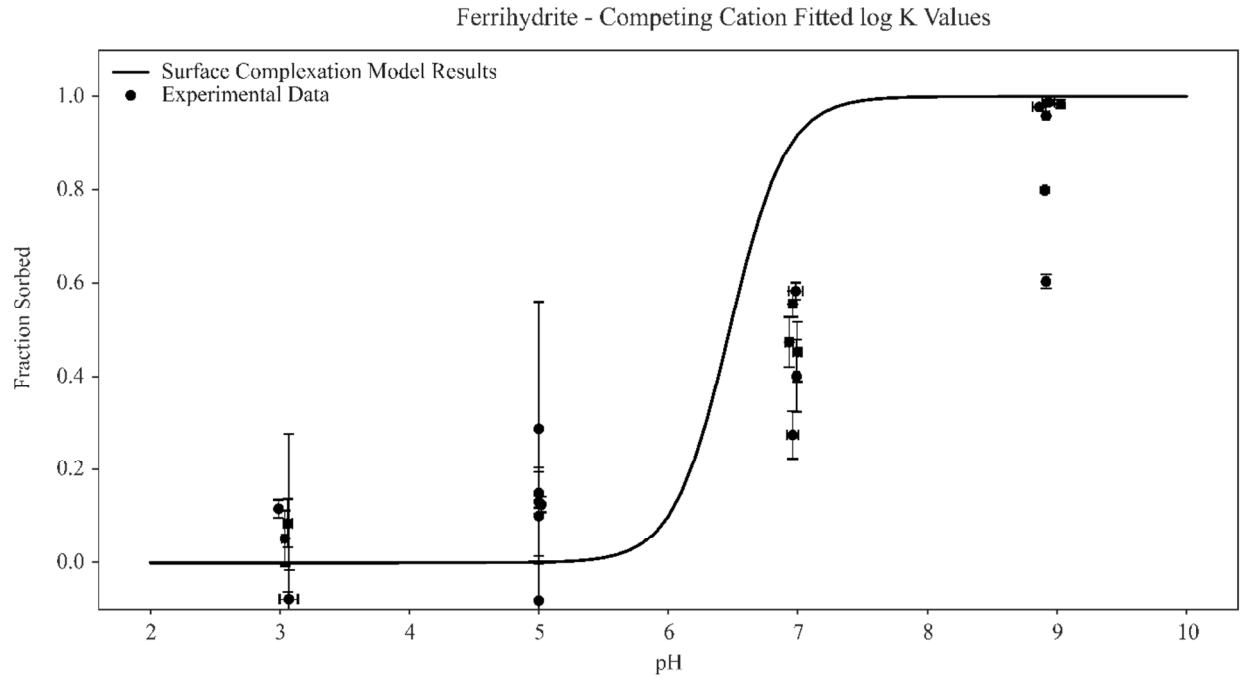

Figure S3: Comparison of ferrihydrite SCM results generated from either fitting isotherm data or fitting competing cation data. Experimental data plotted is from the isotherm experiments with 10 mM NaCl background.

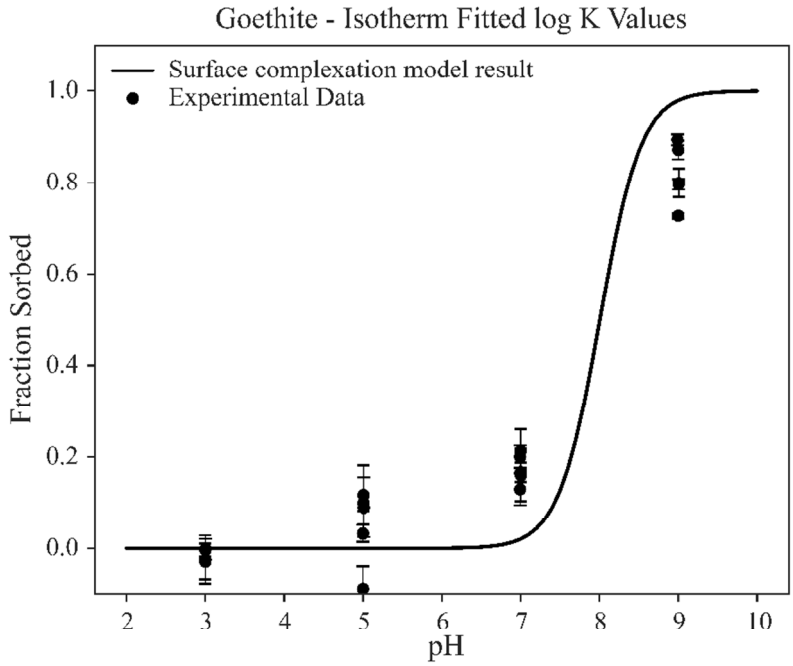

178

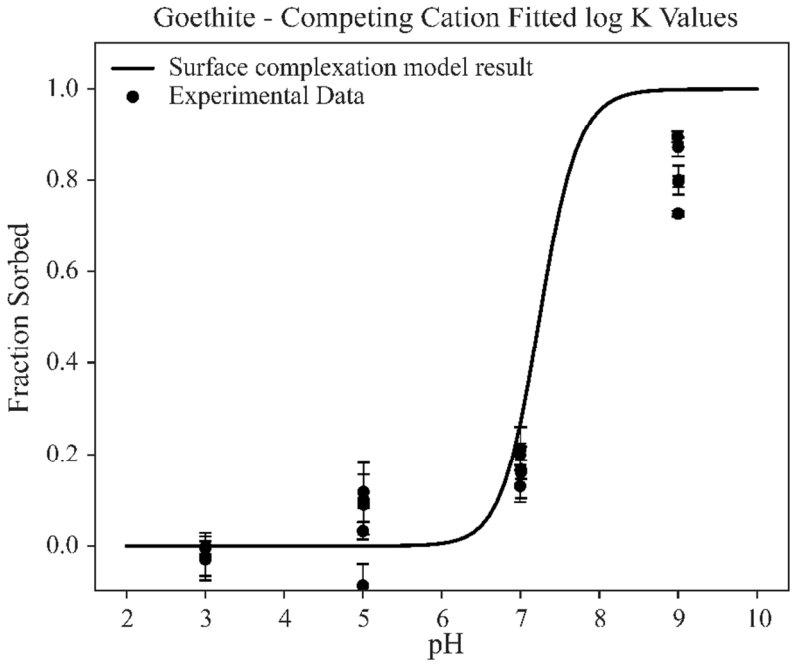

179

180

181 Figure S4: Comparison of goethite SCM results generated from either fitting isotherm data or
182 fitting competing cation data. Experimental data plotted is from the isotherm experiments with
183 10 mM NaCl background.

184

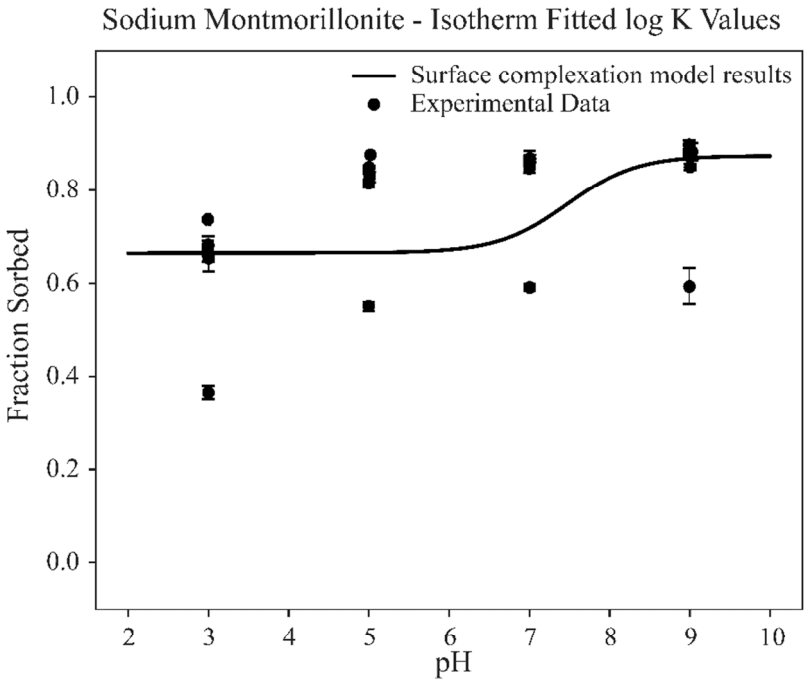

185

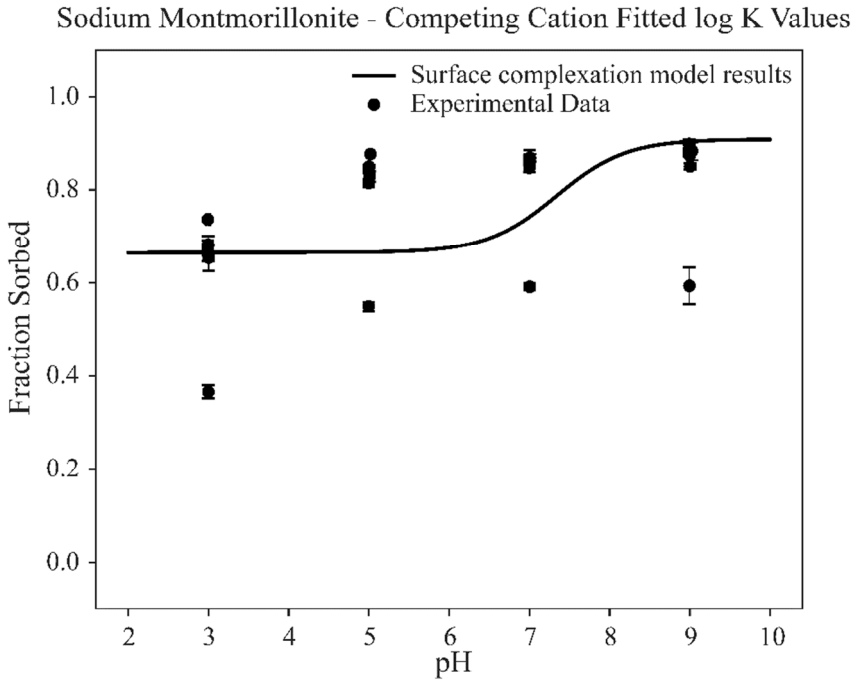

186

187 Figure S5: Comparison of sodium montmorillonite SCM results generated from either fitting
188 isotherm data or fitting competing cation data. Experimental data plotted is from the isotherm
189 experiments with 10 mM NaCl background.

190

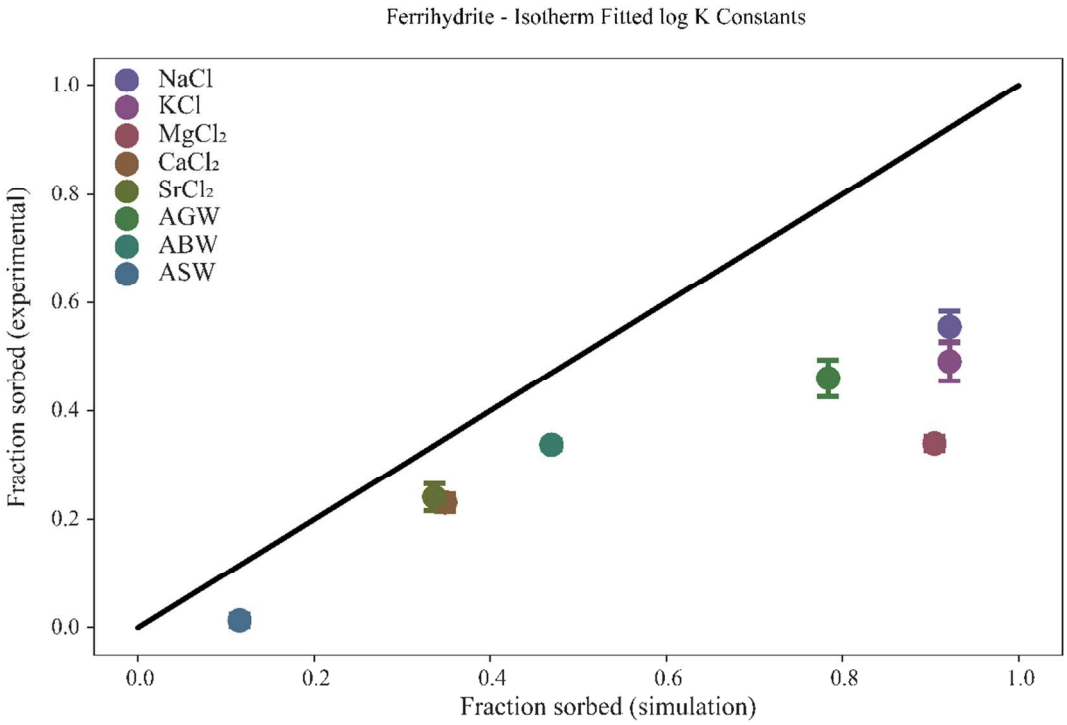

191

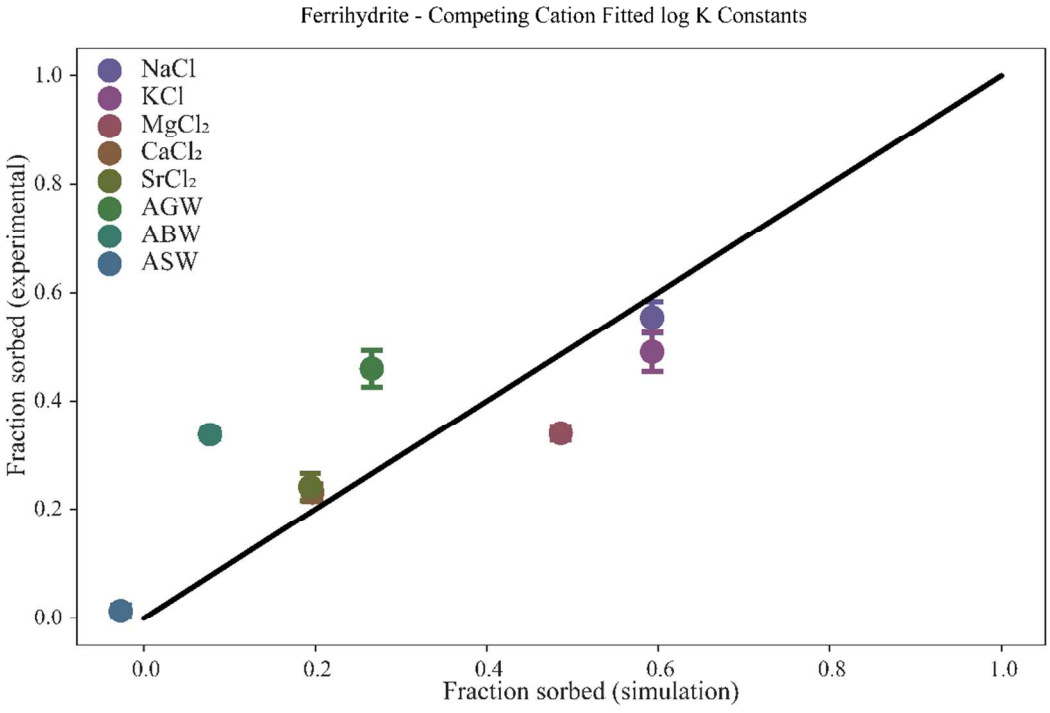

192

193 Figure S6: Ferrihydrite SCM results from either fitting to isotherm data or competing cation data.
194 The simulation results are compared against the relevant competing cation expeirments.

195

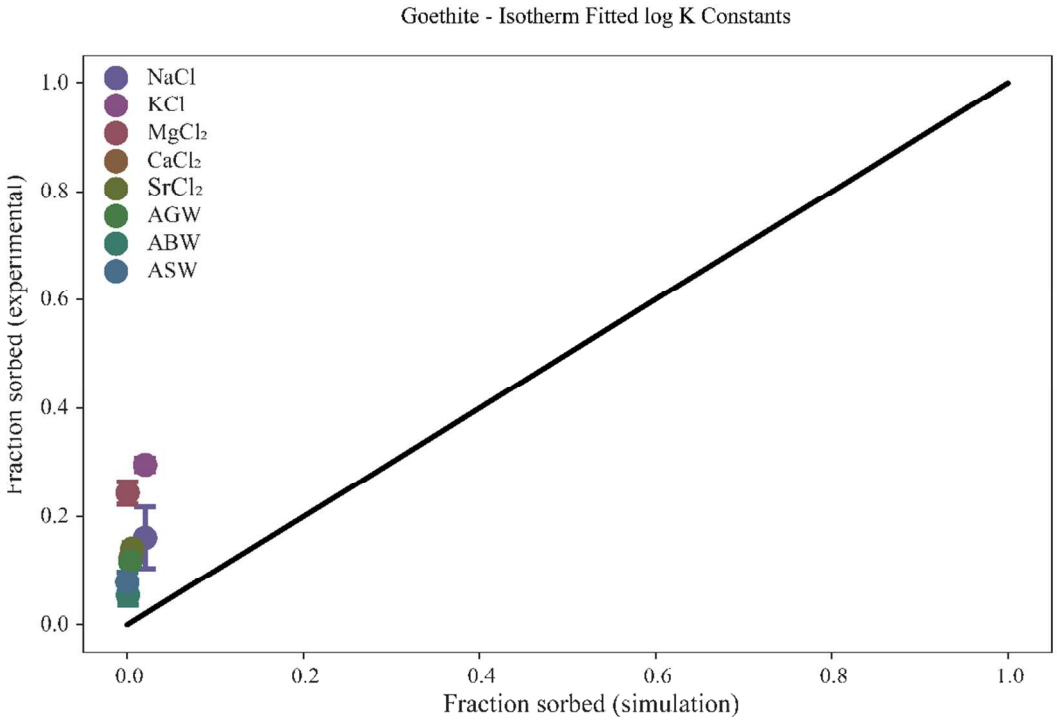

196

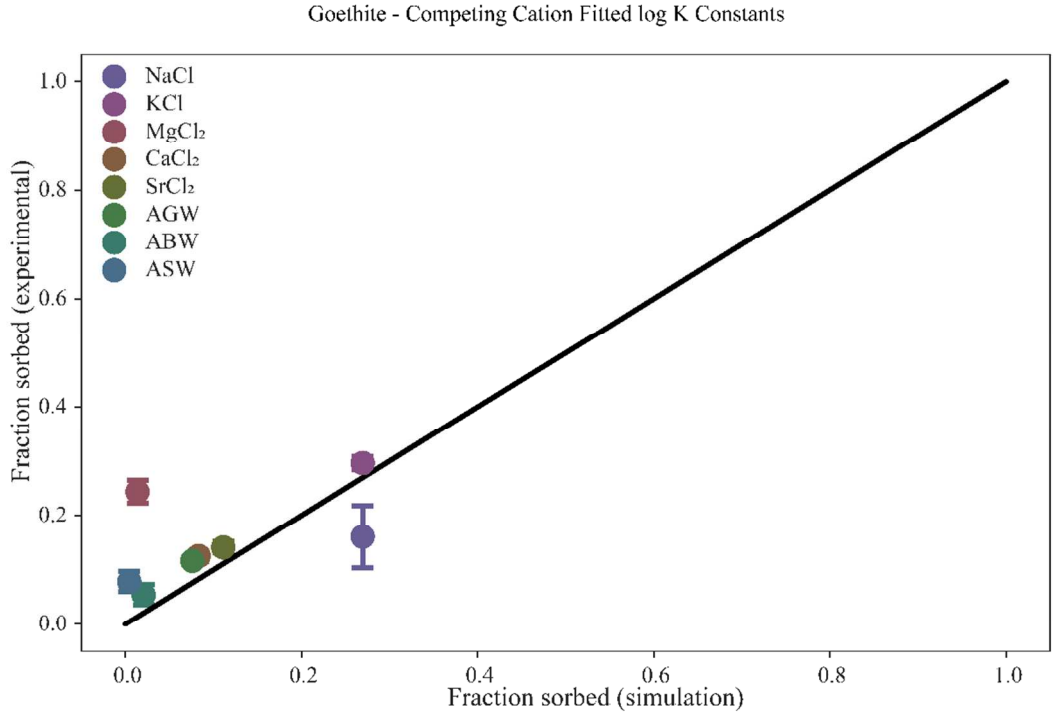

197

198 Figure S7: Goethite SCM results from either fitting to isotherm data or competing cation data.
199 The simulation results are compared against the relevant competing cation expeirments.

200

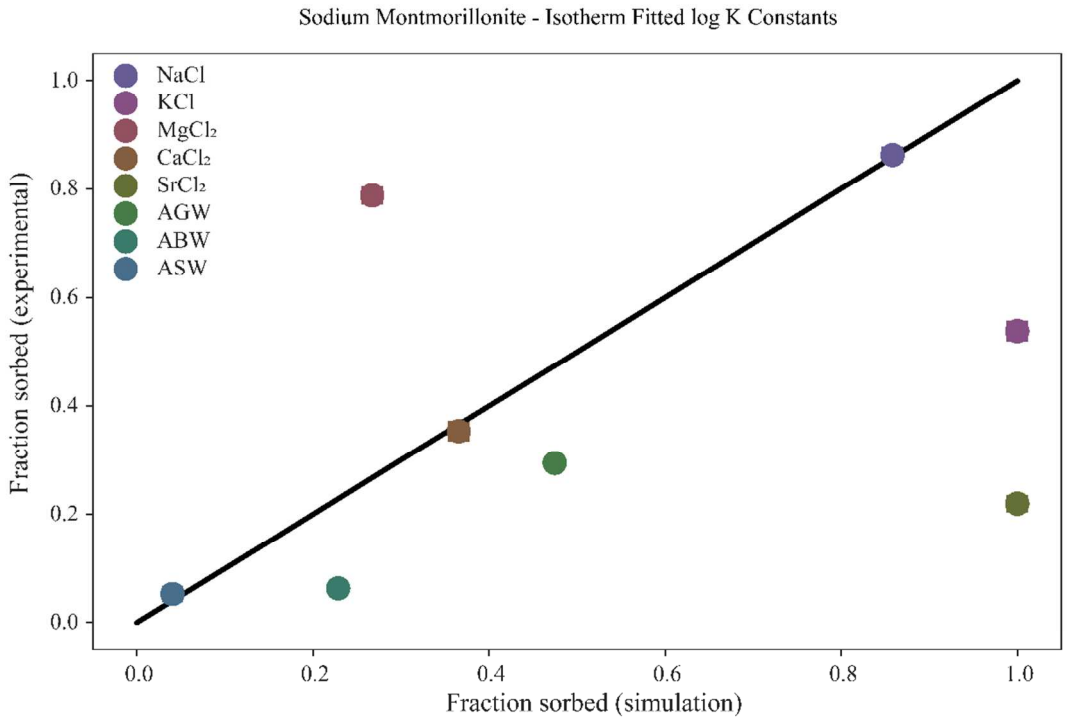

201

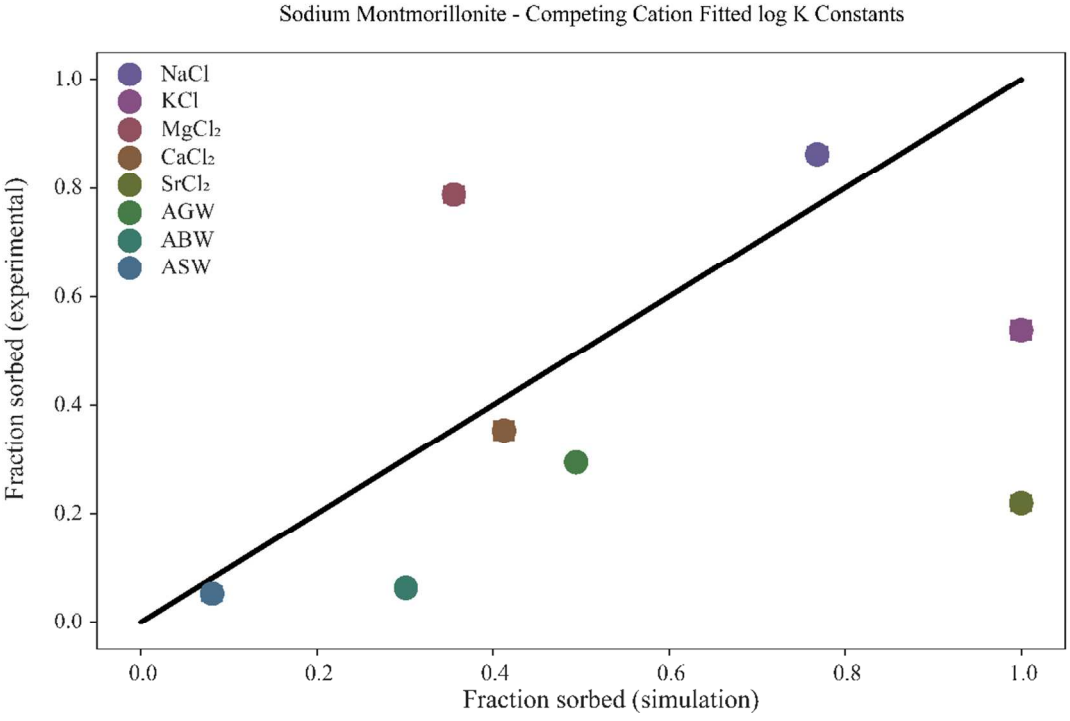

202

203 Figure S8: Sodium Montmorillonite SCM results from either fitting to isotherm data or
204 competing cation data. The simulation results are compared against the relevant competing
205 cation expeirments.

206

References

(1) Michel, F. M.; Ehm, L.; Antao, S. M.; Lee, P. L.; Chupas, P. J.; Liu, G.; Strongin, D. R.; Schoonen, M. A. A.; Phillips, B. L.; Parise, J. B. The structure of ferrihydrite, a nanocrystalline material. *Science* **2007**, *316* (5832), 1726–1729 DOI: 10.1126/science.1142525.

(2) Stookey, L. L. Ferrozine---a new spectrophotometric reagent for iron. *Anal. Chem.* **1970**, *42* (7), 779–781 DOI: 10.1021/ac60289a016.

(3) Klute, A.; Kunze, G. W.; Dixon, J. B. Pretreatment for Mineralogical Analysis. In *Methods of Soil Analysis Part 1 - Physical and Mineralogical Methods*; Soil Science Society of America, American Society of Agronomy, 1986.

(4) ASTM Standard D1141-98. Standard Practice for the Preparation of Substitute Ocean Water. ASTM International: West Conshohocken, PA.

(5) United States Environmental Protection Agency. *Definition and Procedure for the Determination of the Method Detection Limit, Revision 2*; Washington, DC, 2016.

(6) Bradbury, M. H.; Baeyens, B.; Geckeis, H.; Rabung, T. Sorption of Eu(III)/Cm(III) on Ca-montmorillonite and Na-illite. Part 2: Surface complexation modelling. *Geochim. Cosmochim. Acta* **2005**, *69* (23), 5403–5412 DOI: 10.1016/j.gca.2005.06.031.

(7) Sajih, M.; Bryan, N. D. D.; Livens, F. R. R.; Vaughan, D. J. J.; Descostes, M.; Phrommavanh, V.; Nos, J.; Morris, K. Adsorption of radium and barium on goethite and ferrihydrite: A kinetic and surface complexation modelling study. *Geochim. Cosmochim. Acta* **2014**, *146*, 150–163 DOI: 10.1016/j.gca.2014.10.008.

(8) Schwertmann, U.; Cornell, R. *Iron Oxides in the Laboratary*; Wiley-VCH Verlag GmbH: Weinheim, Germany, 2000.

(9) Sverjensky, D. A. Prediction of the speciation of alkaline earths adsorbed on mineral surfaces in salt solutions. *Geochim. Cosmochim. Acta* **2006**, *70* (10), 2427–2453 DOI: 10.1016/j.gca.2006.01.006.

(10) Carroll, S. a; Roberts, S. K.; Criscenti, L. J.; O'Day, P. a. Surface complexation model for strontium sorption to amorphous silica and goethite. *Geochem. Trans.* **2008**, *9*, 2 DOI: 10.1186/1467-4866-9-2.

(11) Kraepiel, A.; Keiler, K. C.; Morel, F. M. M. A Model for Metal Adsorption on Montmorillonite. *J. Colloid Interface Sci.* **1999**, *210* (1), 43–54 DOI: 10.1006/jcis.1998.5947.

(12) Tournassat, C.; Grangeon, S.; Leroy, P.; Giffaut, E. Modeling specific ph dependent sorption of divalent metals on montmorillonite surfaces. a review of pitfalls, recent achievements and current challenges. *Am. J. Sci.* **2013**, *313* (5), 395–451 DOI: 10.2475/05.2013.01.

(13) Duster, T. A. An Integrated Approach to Standard Methods, Materials, and Databases for

the Measurements Used To Develop Surface Complexation Models. *Environ. Sci. Technol.* **2016**, *50* (14), 7274–7275 DOI: 10.1021/acs.est.6b02669.

(14) Naveau, A.; Monteil-Rivera, F.; Dumonceau, J.; Catalette, H.; Simoni, E. Sorption of Sr(II) and Eu(III) onto pyrite under different redox potential conditions. *J. Colloid Interface Sci.* **2006**, *293* (1), 27–35 DOI: 10.1016/j.jcis.2005.06.049.

(15) Beck, A. J.; Cochran, M. a. Controls on solid-solution partitioning of radium in saturated marine sands. *Mar. Chem.* **2013**, *156*, 38–48 DOI: 10.1016/j.marchem.2013.01.008.

(16) Nirdosh, I.; Trembley, W.; Johnson, C. Adsorption-desorption studies on the 226Ra-hydrated metal oxide systems. *Hydrometallurgy* **1990**, *24* (2), 237–248 DOI: 10.1016/0304-386X(90)90089-K.

(17) Tamamura, S.; Takada, T.; Tomita, J.; Nagao, S.; Fukushi, K.; Yamamoto, M. Salinity dependence of 226Ra adsorption on montmorillonite and kaolinite. *J. Radioanal. Nucl. Chem.* **2013**, *299* (1), 569–575 DOI: 10.1007/s10967-013-2740-3.

(18) Ames, L.; McGarrah, J.; Walker, B. Sorption of trace constituents from aqueous solutions onto secondary minerals. II. Radium. *Clays Clay Miner.* **1983**, *31* (5), 335–342.

(19) Dzombak, D.; Morel, F. *Surface Complexation Modeling: Hydrous Ferric Oxide*; Wiley: New York, NY, 1990.

(20) Mathur, S. S.; Dzombak, D. A. Surface complexation modeling: Goethite; 2006; pp 443–468.

(21) van Geen, A.; Robertson, A. P.; Leckie, J. O. Complexation of carbonate species at the goethite surface: Implications for adsorption of metal ions in natural waters. *Geochim. Cosmochim. Acta* **1994**, *58* (9), 2073–2086 DOI: 10.1016/0016-7037(94)90286-0.

(22) Tournassat, C.; Ferrage, E.; Poinsignon, C.; Charlet, L. The titration of clay minerals: II. Structure-based model and implications for clay reactivity. *J. Colloid Interface Sci.* **2004**, *273* (1), 234–246 DOI: 10.1016/j.jcis.2003.11.022.

(23) Charlet, L.; Tournassat, C. Fe(II)-Na(I)-Ca(II) cation exchange on montmorillonite in chloride medium: Evidence for preferential clay adsorption of chloride - Metal ion pairs in seawater. *Aquat. Geochemistry* **2005**, *11* (2), 115–137 DOI: 10.1007/s10498-004-1166-5.

(24) Bradbury, M. H.; Baeyens, B. A mechanistic description of Ni and Zn sorption on Part II: modelling. *J. Contam. Hydrol.* **1997**, *27*, 223–248 DOI: 10.1016/S0169-7722(97)00008-9.

(25) Bradbury, M. H.; Baeyens, B. Modelling the sorption of Mn(II), Co(II), Ni(II), Zn(II), Cd(II), Eu(III), Am(III), Sn(IV), Th(IV), Np(V) and U(VI) on montmorillonite: Linear free energy relationships and estimates of surface binding constants for some selected heavy metals and actinide. *Geochim. Cosmochim. Acta* **2005**, *69* (4), 875–892 DOI: 10.1016/j.gca.2004.07.020.